Electronic Supplementary Material (ESI) for Nanoscale Advances.

Computational Approaches to Enhance Charge Transfer and Stability in TPBi-$(PEA)_2PbI_4$ Perovskite Interfaces through Molecular Orientation Optimization

Syed Muhammad Kazim Abbas Naqvi,[a,b] Yanan Zhu,*[b] Hui Long,[b,c] Zahid Nazir,[b] Roman B. Vasiliev, [c] Olga Kulakovich [d] and Shuai Chang *[b]

[a] *School of Materials Science & Engineering, Beijing Institute of Technology, Beijing 100081, China.*

[b] *Platform for Applied Nanophotonics, Faculty of Materials Science, Shenzhen MSU-BIT University, Shenzhen 518115, China.*

[c] *Department of Materials Science, Department of Chemistry, Lomonosov Moscow State University, Moscow 119991, Russia*

[d] *Institute of Physics of the National Academy of Sciences of Belarus, Minsk 220072, Belarus*

*Corresponding author: Yanan Zhu (zhuyn@smbu.edu.cn); Shuai Chang (schang@smbu.edu.cn)

Binding Energy

The binding energy serves as a critical parameter for comprehending interactions between layers, elucidating the strength of their attachment. A negative binding energy signifies an energy gain or stabilization at the interfacial regions, indicating a favorable interaction and bonding affinity, as previously documented in research.[1] The binding energy values for the TPBi-$(PEA)_2PbI_4$ interface, as outlined in Table S1 and graphically depicted in Fig. S1, play a pivotal role in evaluating the thermodynamic stability of hetero-interfaces. The variations in binding energy values can be attributed to changes in the number of atoms involved in strong interactions when adjusting the TPBi orientation. This adjustment influences the strength of van der Waals interactions between the layers, as illustrated in Fig. 1. The analysis of binding energy across different TPBi orientations interacting with the $(PEA)_2PbI_4$ perovskite surface underscores the significant impact of heterostructure morphology on interface stabilization energy and intermolecular interactions. In Table S1, the binding energy values for TPBi-$(PEA)_2PbI_4$ heterostructures consistently display negative values, indicating strong and favorable interactions for all selected TPBi orientations. This observation contrasts with our previous study,[2] where positive binding energies were noted for 0-degree (horizontal) and 90-degree (vertical) orientations. Notably, the 15-degree and 30-degree TPBi orientations exhibit robust binding energies, emphasizing the influence of heterostructure morphology on enhancing interface stability.

Conversely, the consistently least negative binding energies observed in the 90-degree TPBi orientation indicate weaker interactions, highlighting the distinct behaviour of TPBi-$(PEA)_2PbI_4$ versus TPBi-$FAPbI_3$ heterostructures. This insight provides valuable considerations regarding the influence of material choice on interface stability, particularly in PeLEDs. The study's findings highlight the 15-degree and 30-degree TPBi orientations in TPBi-$(PEA)_2PbI_4$ heterostructures, offering a highly stable interface. This implies the presence of robust chemical bonding, potentially involving covalent or coordinated covalent interactions, thereby contributing to the overall excellence of the interface. Various factors, including surface dipoles, interfacial interactions arising from differences in electronegativity, and polarization effects at the interface, continue to influence the observed effects. Furthermore, the potential for surface reconstruction or material intermixing to generate new, favorable bonding configurations at the interfaces is a critical consideration.

The binding energy of the TPBi-$(PEA)_2PbI_4$ interface was computed using the formula:[3,4]

$$E_b = E_{TPBi-(PEA)_2PbI_4} - (E_{TPBi} + E_{(PEA)_2PbI_4})$$

where $E_{TPBi-(PEA)_2PbI_4}$ represents the energy of the $TPBi-(PEA)_2PbI_4$ interface, while E_{TPBi} and $E_{(PEA)_2PbI_4}$ correspond to the energies of isolated $TPBi$ and isolated $(PEA)_2PbI_4$, respectively.

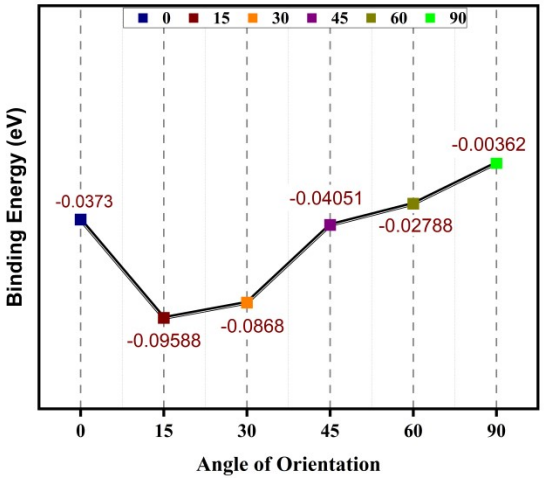

Fig. S1 Binding energy with varying orientations of TPBi.

Computational Details

In exploring the TPBi-$(PEA)_2PbI_4$ interface, we initiated the process by constructing a 2 × 2 × 1 supercell of $(PEA)_2PbI_4$. This supercell was initially created, and a surface was cleaved along the (0 1 0) plane. Subsequently, a vacuum space

measuring 20 Å was introduced. Within this vacant space, the TPBi structure was placed in six different orientations. These orientations were meticulously selected to ensure a comprehensive investigation. The optimized TPBi structure was then carefully situated on the $(PEA)_2PbI_4$ supercell. This intricate procedure aimed to construct the TPBi-$(PEA)_2PbI_4$ interface and guarantee its suitability for creating the desired heterostructures. The TPBi-$(PEA)_2PbI_4$ interface optimization was conducted using the VASP software, applying the Perdew–Burke–Ernzerhof (PBE) exchange-correlation functional.[5] In the case of the 0-degree (horizontal) and 90-degree (vertical) orientations, reference was made to the central benzene ring. In contrast, for the other four orientations, the dihedral angle between the surface atoms of $(PEA)_2PbI_4$ and the nearest ring of TPBi served as the basis for orientation, considering 0-degree orientation as reference. Structural relaxation of all six heterostructures was carried out through the conjugate gradient method within the VASP framework, using the PBE-GGA potential.[6] The optimization process continued until the Hellmann–Feynman force reached a level lower than 0.02 eV/Å. Following the structural relaxation of the heterostructures, a self-consistent calculation was performed using the PBE-GGA exchange-correlation functional. A convergence criterion of 1×10^{-8} eV was employed for this calculation. The process was further refined with a cutoff energy of 550 eV and a Monkhorst-Pack K-point mesh grid of $2 \times 2 \times 1$.[7] The inclusion of the Gaussian smearing method with a 0.1 smearing width ensured the convergence of energy between successive self-consistent electronic cycles. Finally, various post-processing scripts were employed to gain a comprehensive understanding of the charge transfer characteristics of the considered heterostructures. These scripts facilitated the visualization of Density of States (DOS), the projected density of states (PDOS), isosurface charge density, integrated charge density, and Bader Charge analysis.[8]

Supporting Figures

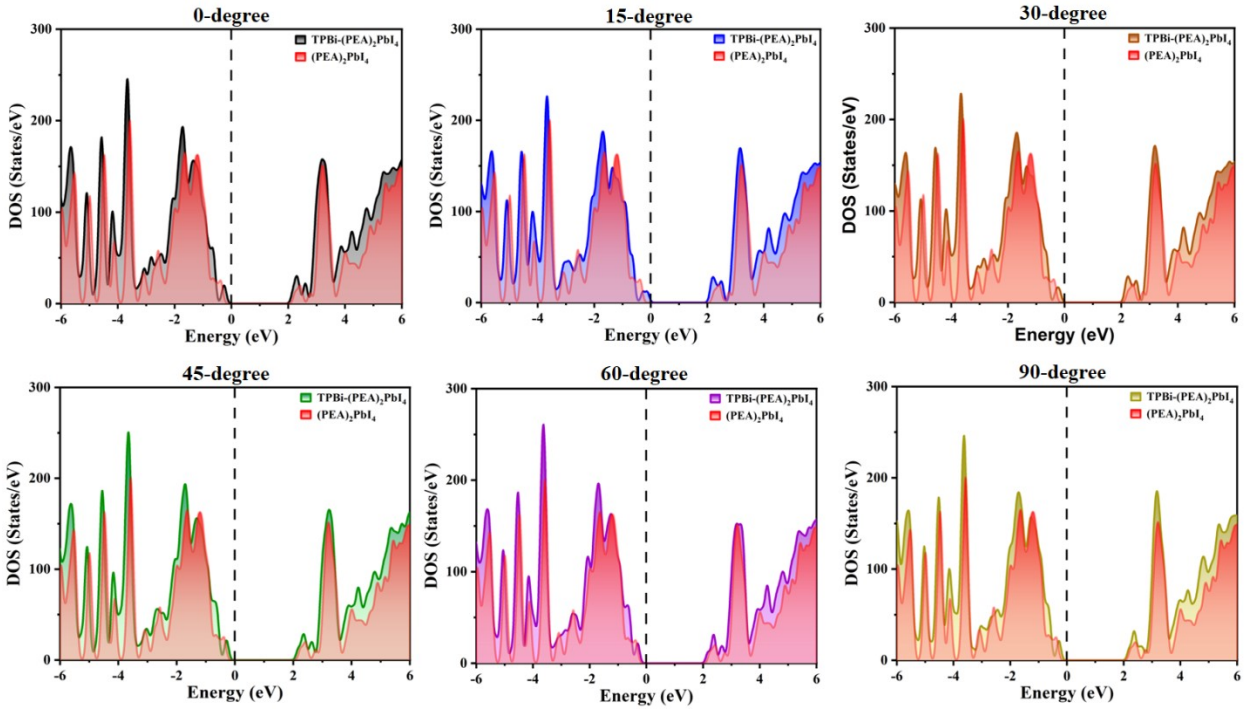

Fig. S2 DOS of TPBi-$(PEA)_2PbI_4$ heterostructures for 0-degree, 15-degree, 30-degree, 45-degree, 60-degree, and 90-degree orientations of TPBi.

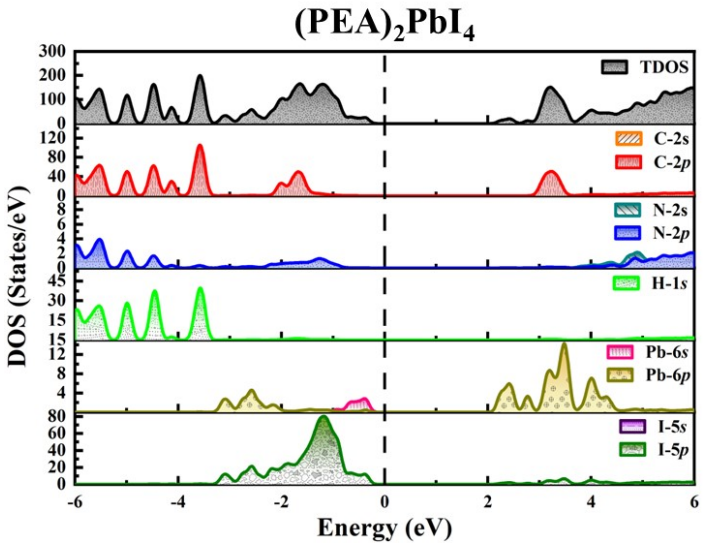

Fig. S3 PDOS of $(PEA)_2PbI_4$ surface without TPBi.

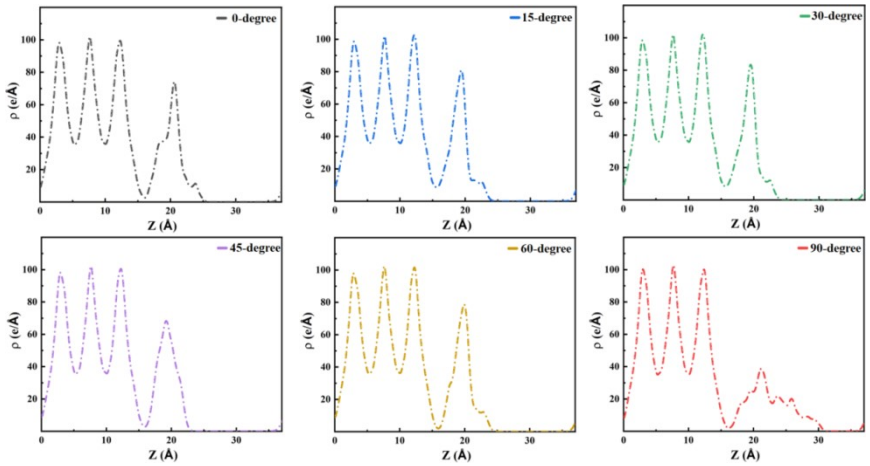

Fig. S4 Charge density profiles for TPBi-$(PEA)_2PbI_4$ interfaces, revealing the distribution of electrons and holes along the z-axis for a comprehensive understanding of charge transfer characteristics..

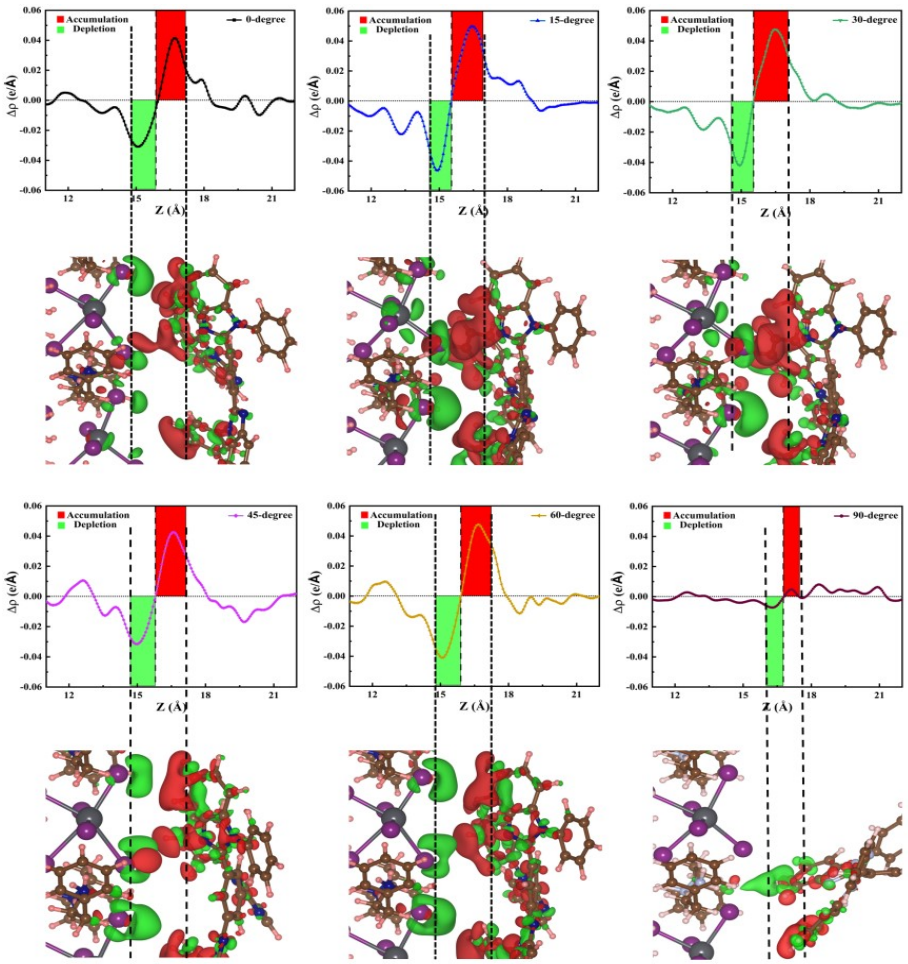

Fig. S5 Charge density difference and interface breakdown for TPBi-$(PEA)_2PbI_4$ interfaces, coupled with Bader charge analysis. Red indicates charge accumulation, green signifies depletion, offering insights into charge transfer dynamics for each orientation.

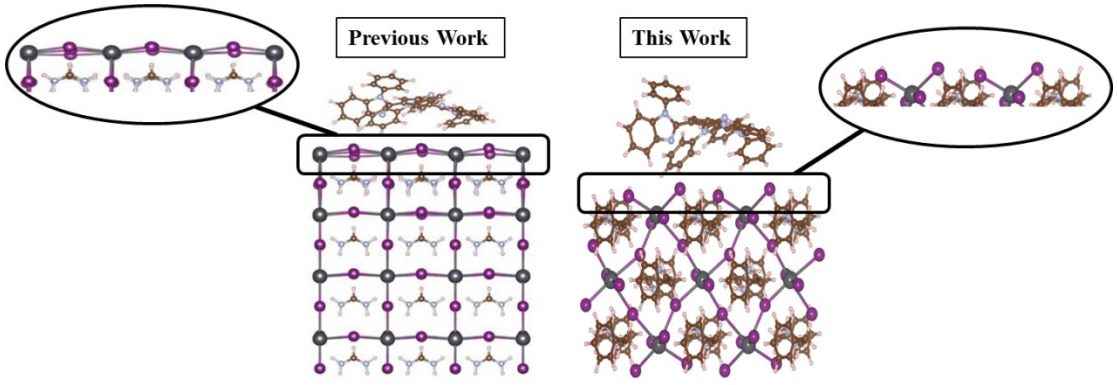

Fig. S6 Comparative analysis of the TPBi-$(PEA)_2PbI_4$ interface with the TPBi-$FAPbI_3$ interface, shedding light on distinctive charge transfer characteristics.

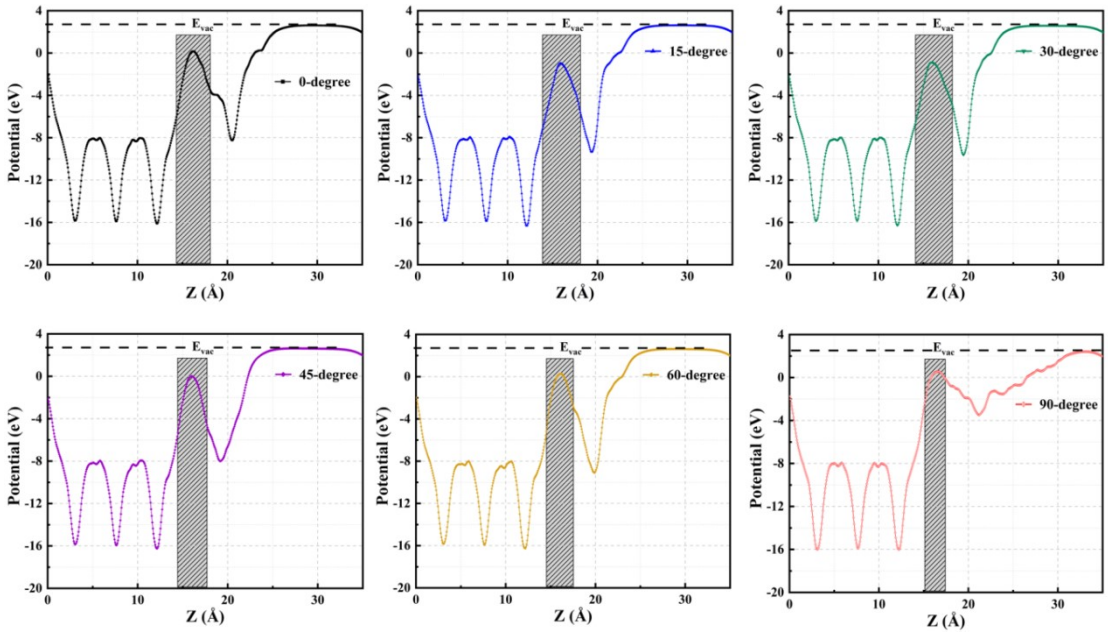

Fig. S7 Electrostatic potential profiles corresponding to each TPBi orientation on the $(PEA)_2PbI_4$ surface, offering insights into the charge transfer dynamics at the TPBi-$(PEA)_2PbI_4$ interfaces.

Supporting Tables

Table S1. The distance of the central ring of TPBi and charge transfer, and binding energy for each structure. (Distance from closest atom = 2Å)

Orientation of TPBi	Distance from central ring (Å)	Charge transfer (e)	Binding Energy (eV)
0-degree	6.1	0.318	-0.037
15-degree	5.2	0.403	-0.096
30-degree	5.3	0.399	-0.087
45-degree	5.4	0.389	-0.041
60-degree	5.9	0.401	-0.028
90-degree	5.7	0.0345	-0.004

Table S2. The Bandgap calculated between the valance band states and conduction band states at the left and right sides from the Fermi level of DOS plots for TPBi-$(PEA)_2PbI_4$ heterostructures.

Orientation	Bandgap	Valence band	Conduction band
0-degree	2.10	-0.08	2.02
15-degree	1.99	0	1.99
30-degree	2.07	-0.05	2.02
45-degree	2.15	-0.12	2.03
60-degree	2.16	-0.14	2.02
90-degree	2.12	-0.09	2.05

REFERENCES

1 Gélvez-Rueda, M. C.; Fridriksson, M. B.; Dubey, R. K.; Jager, W. F.; van der Stam, W.; Grozema, F. C. Overcoming the Exciton Binding Energy in Two-Dimensional Perovskite Nanoplatelets by Attachment of Conjugated Organic Chromophores. *Nat. Commun.* **2020**, *11* (1), 1901.

2 Naqvi, S. M. K. A.; Zhu, Y.; Chang, S. Manipulating Interfacial Performance of TPBi–$FAPbI_3$ Perovskite Interfaces Based on TPBi Orientations: A Theoretical Perspective. *J. Phys. Chem. C* **2023**, *127* (46), 22752–22759.

3 Li, D.; Li, D.; Yang, A.; Zhang, H.; Lai, X.; Liang, C. Electronic and Optical Properties of van Der Waals Heterostructures Based on Two-Dimensional Perovskite $(PEA)_2PbI_4$ and Black Phosphorus. *ACS Omega* **2021**, *6* (32), 20877–20886.

4 Geng, W.; Tong, C.-J.; Liu, J.; Zhu, W.; Lau, W.-M.; Liu, L.-M. Structures and Electronic Properties of Different $CH_3NH_3PbI_3/TiO_2$ Interface: A First-Principles Study. *Sci. Rep.* **2016**, *6* (1), 20131.

5 Tao, J.; Perdew, J. P.; Tang, H.; Shahi, C. Origin of the Size-Dependence of the Equilibrium van Der Waals Binding between Nanostructures. *J. Chem. Phys.* **2018**, *148* (7), 074110.

6 Ziesche, P.; Kurth, S.; Perdew, J. P. Density Functionals from LDA to GGA. *Comput. Mater. Sci.* **1998**, *11* (2), 122–127.

7 Monkhorst, H. J.; Pack, J. D. Special Points for Brillouin-Zone Integrations. *Phys. Rev. B* **1976**, *13* (12), 5188–5192.

8 Tang, W.; Sanville, E.; Henkelman, G. A Grid-Based Bader Analysis Algorithm without Lattice Bias. *J. Phys. Condens. Matter* **2009**, *21* (8), 084204.